HHS Public Access

Author manuscript

Exp Eye Res. Author manuscript; available in PMC 2018 September 01.

Published in final edited form as:

Exp Eye Res. 2017 September ; 162: 129–138. doi:10.1016/j.exer.2017.07.008.

Direct Measurement of Pressure-Independent Aqueous Humour Flow using *iPerfusion*

Michael Madekurozwa[a], **Ester Reina-Torres**[a], **Darryl R. Overby**[a,*], and **Joseph M. Sherwood**[a]

[a]Dept. of Bioengineering, Imperial College London, London, SW7 2AZ, UK

Abstract

Reduction of intraocular pressure is the sole therapeutic target for glaucoma. Intraocular pressure is determined by the dynamics of aqueous humour secretion and outflow, which comprise several pressure-dependent and pressure-independent mechanisms. Accurately quantifying the components of aqueous humour dynamics is essential in understanding the pathology of glaucoma and the development of new treatments. To better characterise aqueous humour dynamics, we propose a method to directly measure pressure-independent aqueous humour flow. Using the *iPerfusion* system, we directly measure the flow into the eye when the pressure drop across the pressure-dependent pathways is eliminated. Using this approach we address i) the magnitude of pressure-independent flow in *ex vivo* eyes, ii) whether we can accurately measure an artificially imposed pressure-independent flow, and iii) whether the presence of a pressure-independent flow affects our ability to measure outflow facility. These studies are conducted in mice, which are a common animal model for aqueous humour dynamics. In eyes perfused with a single cannula, the average pressure-independent flow was 1 [−3, 5] nl/min (mean [95% confidence interval]) (N=6). Paired *ex vivo* eyes were then cannulated with two needles, connecting the eye to both *iPerfusion* and a syringe pump, which was used to impose a known pressure-independent flow of 120 nl/min into the experimental eye only. The measured pressure-independent flow was then 121 [117, 125] nl/min (N=7), indicating that the method could measure pressure-independent flow with high accuracy. Finally, we showed that the artificially imposed pressure-independent flow did not affect our ability to measure facility, provided that the pressure-dependence of facility and the true pressure-independent flow were accounted for. The present study provides a robust method for measurement of pressure-independent flow, and demonstrates the importance of accurately quantifying this parameter when investigating pressure-dependent flow or outflow facility.

Keywords

Aqueous humour dynamics; iPerfusion; unconventional outflow; uveoscleral outflow; pressure-independent flow; outflow facility; ocular biomechanics

*Corresponding author: d.overby@imperial.ac.uk.

1. Introduction

Glaucoma is a world leading cause of irreversible blindness (Resnikoff et al., 2004) and elevated intraocular pressure (IOP) is the major risk factor. IOP reduction is the sole clinical objective to prevent further glaucomatous vision loss, regardless of whether IOP is elevated (Van Veldhuisen et al., 2000). Understanding the physiology of IOP regulation, and its dysregulation in glaucoma, is therefore central to developing and evaluating new IOP-lowering therapies.

IOP is determined by a mass balance between aqueous humour secretion into the eye (Q_{in}), and aqueous humour outflow, via pressure-independent mechanisms (Q_u) and pressure-dependent mechanisms (characterised by the outflow facility C). A mass balance of the flows entering and exiting the eye yields a form of what is known as Goldmann's equation:

$$Q_{in}+Q=C\,(P-P_e)+Q_u \quad (1)$$

which includes an additional term representing inflow from a perfusion system (Q). P and P_e represent IOP and episcleral vessel pressure respectively. Most treatments for glaucoma aim to reduce Q_{in} or increase Q_u, with a number of new treatments targeting C (Stamer and Acott, 2012). IOP elevation in glaucoma is attributed to reduced values of C (Grant, 1951). Studies of aqueous humour dynamics (AHD) therefore aim to measure the various parameters of Eq. 1 so as to elucidate the factors controlling IOP.

Mice are common models to study AHD (Aihara et al., 2003; Boussommier-Calleja et al., 2012; Crowston et al., 2004; Lei et al., 2011; Li et al., 2016; Millar et al., 2011; 2015; Toris et al., 2016; Zhang et al., 2002; Zhang et al., 2009). However, some studies report that as much as 60–80% of outflow is pressure-independent in young mice (Aihara et al., 2003; Crowston et al., 2004; Lei et al., 2011), although the fraction of pressure-independent outflow may decrease with age (Millar et al., 2015). This contrasts with humans, where the majority of outflow is pressure-dependent (Bill and Phillips, 1971; Toris et al., 1995; Townsend and Brubaker, 1980), although reported values of the exact proportion vary over a large range, as reviewed by Johnson et al. (2017). If pressure-independent outflow truly dominates in mice, then the validity of mouse models for AHD becomes questionable.

Pressure-independent outflow (Q_u) in post-mortem mice has generally been estimated indirectly by linear extrapolation to estimate the flow rate when $P = P_e$, under conditions where Q_{in} is eliminated (Lei et al., 2011; Millar et al., 2011). In living mice, Q_u has been estimated indirectly by solving Goldmann's equation after measuring C, P_e, Q_{in} and spontaneous IOP (Aihara et al., 2003). Alternatively, the quantity of unconventional (i.e. non-trabecular) outflow has been estimated in living mice based on accumulation of tracer in the uveoscleral tissues (Millar et al., 2011). As unconventional outflow is typically assumed to exhibit pressure-insensitivity, it is often equated with Q_u, although this assumption is questionable (Johnson et al., 2017).

Here, we present a method to *directly* measure the *net pressure-independent flow*, Q_0, defined as the difference between pressure-independent inflow and outflow according to

$$Q_0 = Q_{in} - Q_u \quad (2)$$

To measure Q_0, we cannulate the anterior chamber with a needle and interface the eye with the *iPerfusion* system (Sherwood et al., 2016) that allows direct measurement of Q for a prescribed value of P. By setting $P = P_e$, the pressure-dependent component of outflow is eliminated (see Eq. 1), enabling a direct measurement of Q_0. Note that $P_e = 0$ in an enucleated eye.

This report addresses the following questions:

1. What is the magnitude of pressure-independent flow, Q_0, in enucleated mouse eyes?
2. If pressure-independent flow were present ($Q_0 \neq 0$), as *in vivo*, could it be measured accurately using *iPerfusion*?
3. Does non-zero pressure-independent flow affect the measurement of outflow facility?

2. Material and Methods

2.1 Experimental Design

To answer Question 1, we cannulated enucleated mouse eyes with a single cannula connected to *iPerfusion*, as shown in Fig. 1. Following a standard perfusion protocol to ensure that the ocular response was normal, the applied pressure was set to zero and the flow rate Q into the eye was measured as P approached zero. To answer Question 2, we cannulated enucleated mouse eyes with two cannulae, providing connections to both *iPerfusion* and a syringe pump (see Fig. 1). The syringe pump was used to impose a known pressure-independent flow directly into one eye. We then asked whether *iPerfusion* was able to resolve this additional flow rate by direct measurement of Q as P approached zero. To answer Question 3, we compared outflow facility measurements between contralateral eyes, with one eye receiving the imposed pressure-independent flow. As outflow facility is tightly correlated between contralateral enucleated eyes of an individual mouse (Sherwood et al., 2016), a systematic offset in the facility between paired eyes would indicate that the magnitude of pressure-independent flow affects the measurement of facility.

2.2 Detailed Methods

2.2.1 Animal Husbandry—Eyes were obtained from male C57BL/6 mice (Charles River UK, Ltd) aged 9–16 weeks. All mice were housed in clear cages at 21°C with a 12-hour light-dark cycle (lights on at 7 AM). Food and water were supplied *ad libitum*. Mice were euthanised by cervical dislocation and eyes were enucleated and stored in PBS at room temperature for no more than 1 hour prior to cannulation. The time between death and completion of the perfusion did not exceed 5.5 hours. All experiments were performed in accordance with the ARVO Statement for the Use of Animals in Ophthalmic and Vision

Research. Experiments were conducted under the authority of a UK Home Office Project Licence.

2.2.2 Ocular Perfusion Setup—Enucleated eyes were fixed to a platform with a small amount of cyanoacrylate glue (Loctite Precision Super Glue, Henkel, UK) and fully submerged in a bath of PBS maintained at 35.0 ± 0.5 °C for the duration of the experiment. Glass needles mounted on micromanipulators were used to cannulate the anterior chamber of the eye under a stereomicroscope. The needles were made by pulling borosilicate glass pipettes (B100-50, Sutter Instrument, USA) in a laser puller (P2000, Sutter Instrument) and were bevelled in a pipette beveller (SYS-48000, WPI, USA) to a 45° tap er and a 100 μm outer diameter at the tip. The perfusate used in both cannulae was Dulbecco's PBS with 5.5 mM glucose passed through a sterile 0.22 μm filter prior to use. The flow rate from the *iPerfusion* system into the eye, Q, at pressure P was measured as described previously (Chandrawati et al., 2017; Li et al., 2016; O'Callaghan et al., 2017; Reina-Torres et al., 2017; Sherwood et al., 2016; Tam et al., 2017; Wang et al., 2017). As shown in Fig. 1, *iPerfusion* comprises an actuated pressure reservoir used to control P_a and a thermal flow sensor (SLG64, Sensirion, Switzerland) to measure Q. The pressure within the eye relative to the water bath (P) is measured using a differential pressure sensor (PX409, Omegadyne, USA). In the double cannula experiments, the second needle was connected to a 50 μl glass syringe (Gastight, Hamilton, USA), mounted on a syringe pump (PHD Ultra, Harvard Apparatus, USA). Supplementary Information provides an evaluation of the pump performance measured using the flow sensor.

The thermal flow sensor measures Q through a 75 μm glass capillary, which has a hydrodynamic resistance (R_q) in the range 8–10 mmHg/(μl/min) (measured prior to each perfusion). The pressure in the eye (P) thus differs from the applied reservoir pressure (P_a) according to:

$$P = P_a - R_q Q \quad (3)$$

Eq. 3 can be used to set the value of P_a in order to achieve a desired P.

The hydrodynamic resistance of the needles, measured prior to each perfusion, was always < 0.2 mmHg/(μl/min). Even at a high flow rate of 200 nl/min, this would result in a pressure drop of < 0.04 mmHg, which is within the resolution of the pressure sensor. The pressure drop across the needle was therefore neglected.

2.2.3 Single Cannula Experiments—Single eyes from individual mice (N=6) were cannulated with a single needle and underwent a 9-step pressure perfusion following previous methods (Sherwood et al., 2016). Briefly, following acclimatisation at 8 mmHg for 30 minutes, the eye was perfused at 9 pressure steps between 4.5 and 21 mmHg. We then measured the flow rate as the pressure approached zero, termed $Q(P \rightarrow 0)$. The approach to zero pressure is asymptotic because the compliance of the eye, as described by Friedenwald's model (Friedenwald, 1937), is given by $1/KP$, where K is the ocular rigidity. Hence the compliance tends towards very high values at low pressures, and larger

compliances increase the time to reach steady state. To reduce the time to reach steady state, P was set to 2 mmHg with the flow sensor bypassed (thereby setting $R_q = 0$ in Eq. 3), instantaneously setting the pressure in the eye to P_a. The flow bypass was then closed, and the applied pressure was set to 0 mmHg. Steady state was defined as when the rate of change of P, calculated by linear regression over a 5 minute window, was less than 0.01 mmHg/min continuously for 1 minute. The mean and standard deviation of Q and P for the pressure step were calculated from the final 4 minutes of data.

2.2.4 Double Cannula Experiments—In these experiments, an artificial pressure-independent flow was imposed through the second cannula using the syringe pump (Fig. 1). The imposed flow rate into the eye was defined to be $Q_p = 120$ nl/min, chosen to approximate the difference between aqueous humour secretion (~150 nl/min), averaged from previous studies (Aihara et al., 2003; Millar et al., 2015; 2011; Toris et al., 2016) and pressure-independent outflow (~30 nl/min), chosen from the reported range of 0–120 nl/min (Boussommier-Calleja et al., 2012; 2015; Boussommier-Calleja and Overby, 2013; Chang et al., 2015; Kumar et al., 2013; Lei et al., 2011; Li et al., 2014; Overby et al., 2014a; Overby et al., 2014b; Rogers et al., 2013).

Paired eyes (N=7 pairs) were perfused simultaneously on duplicate *iPerfusion* systems, where contralateral eyes received an imposed flow rate of 0 or 120 nl/min. The perfusion protocol consisted of three phases: I) acclimatisation, II) direct measurement of $Q(P \rightarrow 0)$, and III) characterisation of the flow-pressure relationship to measure C. Fig. 2 shows a sample tracing from a pair of eyes.

Phase I: Acclimatisation: During phase I the reservoir pressure was set to $P_a = 9.5$ mmHg for 30 minutes to allow the eye to acclimatise to the perfusion system.

Phase II: Direct measurement of pressure-independent flow: Phase II is indicated by the blue shaded regions in Fig. 2. For the control case, where $Q_p = 0$ nl/min, P_a was set to 0 mmHg (Fig. 2a). For the experimental case where $Q_p = 120$ nl/min, P_a was set to $-R_q Q_p$ (see Eq. 3), using the value of R_q measured prior to the perfusion. A period of 60 minutes was allowed, and the final pressure and $Q(P \rightarrow 0)$ were calculated as the average pressure and flow rate over the final 4 minutes.

Phase III: Measuring outflow facility: The flow-pressure relationship was then evaluated over 5 additional pressure steps, equally spaced in the range $P_a = 3$–15 mmHg. Steady state at each step was determined once the rate of change of Q/P, calculated by linear regression over a 5 minute window, was continuously less than 0.1 nl/min/mmHg/min for 1 minute. The mean and standard deviation of the final 4 minutes were then extracted and defined as the steady state flow rate and pressure for each step (see green regions in Fig. 2 and data points in Fig. 3). In order to estimate the outflow facility, we fit a power law model based on our previous study (Sherwood et al., 2016), but with Q_0 added as a free parameter to allow for pressure-independent flow:

$$Q = C_r (P/P_r)^{\beta} P + Q_0 \quad (4)$$

where C_r is the 'reference facility' at a 'reference pressure' of P_r = 8 mmHg, defined based on the physiological pressure drop between the anterior chamber and episcleral vessels. The exponent β characterises the nonlinearity of the flow-pressure relationship. Eq. 4 was fit to the data using weighted non-linear regression, with weights defined as the reciprocal variance of the flow rate over the 4-minute window for each step. Sample flow-pressure plots with best fits and confidence intervals are given in Fig 3.

2.3 Statistics

Statistics for normally distributed data, such as pressure or flow rate, are reported in the form

$$\overline{Q} \pm ME_{\overline{Q},95}\left(2s_Q\right) \quad (5)$$

where, $\bar{Q}$ is the mean or best fit parameter, $ME_{\bar{Q},95}$ is the 95% margin of error (the half-width of the 95% confidence interval (CI)) and s_Q is the sample standard deviation.

Facility, C, is better represented by a lognormal distribution (Sherwood et al., 2016). Hence the fold change in facility between paired eyes is also lognormally distributed. To account for the multiplicative nature of the lognormal distribution, statistical values of facility, or fold changes in facility, are given in the form

$$\overline{C}^{*\times}/ME_{\overline{C}^*,95}\left(s_C^{*2}\right) \quad (6)$$

where $\bar{C}^*$ is the geometric mean, with 95% margin of error $ME_{\bar{C}^*,95}$ and geometric sample standard deviation s_C^{*2}, as described in our previous study (Sherwood et al., 2016). All statistical analyses on facility were carried out on the log-transformed reference facility, $Y_r = \log(C_r)$, yielding a normally distributed parameter, Y_r, suitable for the t-test.

3. Results

3.1 What is the magnitude of pressure-independent flow in enucleated mouse eyes?

We first measured pressure-independent flow at zero pressure in enucleated mouse eyes. Figs. 4a and b show how the pressure and flow rate asymptotically approached zero after setting P_a = 0 in the single cannula experiments. Fig. 4c shows the steady state flow and pressure values, with each point representing the mean for a given eye and ellipses indicating two standard deviations. The grey bands indicate the measurement uncertainty of the flow and pressure sensors (see Supplemental Information 1 in Sherwood et al. (2016)). For these six eyes, the average $Q(P \rightarrow 0)$ was 1 ± 4 (7) nl/min (see Eq. 5), which was not significantly different from zero (p = 0.44). The average steady state pressure was approximately zero, 0.04 ± 0.04 (0.07) mmHg, within the accuracy of the pressure sensor. This confirms that there is zero pressure-independent flow in enucleated mouse eyes.

3.2 Can *iPerfusion* measure pressure-independent flow when it is present?

Figs. 5a and b show the values of $Q(P\rightarrow 0)$ measured during Phase II of the double cannula experiments. For the experimental eyes (Fig. 5a), in which there was a pressure-independent flow into the eye of Q_p = 120 nl/min, the mean $Q(P\rightarrow 0)$ was −121 ± 4 (8) nl/min with a mean P of 0.11 ± 0.07 (0.14) mmHg. $Q(P\rightarrow 0)$ was insignificantly different from $-Q_p$ (p = 0.58, N=7). Note that the negative value of the measured flow rate indicates net flow out of the eye, as expected. For the control eyes (Fig. 5b), where Q_p = 0 nl/min, the mean $Q(P\rightarrow 0)$ was −10 ± 2 (5) nl/min. The difference between $-Q_p$ and $Q(P\rightarrow 0)$ was small but detectible ($p < 10^{-3}$, N=7), and attributable to the control eyes not having fully reached steady state, as the final mean pressure (0.19 ± 0.02 (0.04) mmHg) had not quite reached zero ($p < 10^{-3}$). Note that for all control eyes, $Q(P\rightarrow 0)$ was negative and therefore cannot be interpreted as pressure independent outflow, which would yield a positive Q.

3.3 Does pressure-independent flow affect facility measured by *iPerfusion*?

Finally, we consider whether the presence of pressure-independent flow, should it exist as *in vivo*, affects measurements of outflow facility. Fig. 6 compares the reference facility C_r, measured in the contralateral control and experimental eyes, where the ellipses represent the 95% confidence bounds on C_r. If an ellipse overlaps the unity line, the difference in facility between the control and experimental eyes of that mouse is not significantly different from zero (equivalent to a fold difference of unity). Analysing all the pairs yields an average fold difference of 0.98 ^{x}/1.27 (1.67) (see Eq. 6), which is not significantly different from unity (p = 0.82, N=7 pairs). The average facility for all 14 eyes was 6.25*/1.14 (1.55) nl/min/mmHg.

4. Discussion

In the present study, we report the first *direct* measurements of *pressure-independent* aqueous humour flow. By equalising the pressure between the eye and the bath, flow across the pressure-dependent pathways was eliminated. This left only pressure-independent flow, Q_0, which represents the difference between inflow and pressure-independent outflow. Using *iPerfusion*, we demonstrated that Q_0 = 0 in enucleated mouse eyes. Further, when a known Q_0 was imposed, we could accurately measure it.

4.1 The absence of pressure-independent flow *ex vivo*

For the *ex vivo* eyes in the present study, aqueous humour secretion would be expected to rapidly approach zero, due to cessation of blood flow. Hence, *ex vivo* measurements of Q_0 would reflect Q_u, the pressure-independent *outflow*. Our direct measurements gave an average Q_0 of 1 ± 4 (7) nl/min (N=6). From this, we conclude that the magnitude of the pressure-independent outflow in enucleated mouse eyes is insignificantly different from zero, and if present has a magnitude of less than ~5 nl/min. This result is in contrast with prior estimates of pressure-independent outflow in C57 mice of similar ages, as estimated by extrapolation in enucleated eyes which vary between 0 to 120 nl/min (Boussommier-Calleja et al., 2015; 2012; Boussommier-Calleja and Overby, 2013; Chang et al., 2015; Kumar et al., 2013; Lei et al., 2011; Li et al., 2014; Overby et al., 2014a; Overby et al., 2014b; Rogers et al., 2013). This indicates that linear extrapolation is not an appropriate method for predicting pressure-independent flow in mouse eyes. Although there is no pressure-independent flow in

enucleated eyes, there are reports suggesting that pressure-independent flow may exist in eyes perfused in situ following death (Millar et al., 2015; 2011). Additionally, insufficient hydration of the corneoscleral shell during a perfusion can result in an evaporative loss that generates an artefactual pressure-independent outflow (Boussommier-Calleja et al., 2015).

4.2 What about uveoscleral outflow?

The absence of pressure-independent flow does not imply that there is no uveoscleral outflow. In contrast to the *functional* description of 'pressure-independent flow' used in this study, uveoscleral outflow is an *anatomical* definition. The uveoscleral outflow pathway comprises flow through gaps in the ciliary muscle, into the supraciliary and suprachoroidal spaces, and thence across the sclera into the extraocular space. Flow through each of these tissues is driven by a pressure gradient, and is hence by definition, pressure-dependent. However, the hydrodynamic resistances of these tissues may vary with pressure.

As flow through the uveoscleral tissues is pressure-dependent, in the absence of a pressure gradient, we would not expect any uveoscleral outflow. At higher pressures, uveoscleral outflow may well occur *ex vivo*, but it is not possible to distinguish anatomical flow routes (i.e. uveoscleral from trabecular outflow) from perfusion measurements alone.

The value of C measured by perfusion combines the influence of trabecular and uveoscleral outflow facilities, along with any other pressure-dependent flow mechanisms, (including pseudofacility: the pressure-dependent decrease in aqueous humour secretion (Becker and Neufeld, 2002; Kaufman, 2003)). *In vivo*, the pressure gradient driving uveoscleral outflow is determined by the intraocular and extraocular pressures, $P - P_0$, in contrast to that for trabecular outflow, which is determined by the difference between the intraocular and episcleral vessel pressures, $P - P_e$. Including these terms in Equation (1) yields a form of the modified Goldmann's equation:

$$Q_{in}+Q=C_{tr}\,(P-P_e)+C_u\,(P-P_o)+C_{ps}\,(P-P_{cc})+Q_u \quad (7)$$

where C_{tr} and C_u are the trabecular and uveoscleral outflow facilities, respectively, C_{ps} is the pseudofacility, P_{cc} is the ciliary processes capillary pressure and Q_u represents any pressure-independent outflow that may be present *in vivo*, such as that due to uveovortex outflow. For enucleated eyes, there is no aqueous humour production ($Q_{in} = 0$, $C_{ps} = 0$), zero pressure-independent outflow ($Q_u = 0$), and extraocular and episcleral vessel pressures are equal to the external reference pressure. Equation 7 thus reduces to:

$$Q=(C_{tr}+C_u)\,P$$

4.3 How does Q_0 affect our interpretation of flow-pressure data?

Pressure-independent outflow has typically been interpreted as the intercept from a linear fit to the flow-pressure data. This ostensibly represents the outflow rate when the pressure drop across all pressure-dependent pathways is eliminated. What has not generally been recognised is that this interpretation has a considerable impact on the assessment of outflow

facility. To demonstrate this Figs. 7a–c show different fits to a representative flow-pressure data set, artificially generated based on the average values from *iPerfusion* measurements of 66 C57 mice (C_r = 5.5 nl/min/mmHg, β = 0.66) (Sherwood et al., 2016). A normally distributed random noise was applied to the flow rates with a standard deviation of 3 nl/min, consistent with previous *iPerfusion* data (see Supplementary Information 1 in Sherwood et al. (2016)).

Fig. 7a shows the common linear fit (with a finite Q_0 as a free parameter). For this representative case, the fit yields Q_0 = −50 [−60,−32] nl/min (mean [95% CI]), and C_r = 12.0 [10.5, 13.6] nl/min/mmHg. However, as we have demonstrated that Q_0 = 0, this fit is clearly not appropriate, as the estimated value of Q_0 is significantly different from zero. If one enforces Q_0 = 0, but still imposes a linear fit (thereby implicitly defining a constant facility, see Fig. 7b), the model is clearly not appropriate as it does not capture the form of the data. Hence, it must be concluded that the facility itself is a function of pressure for these measurements. A power law model of the form of Eq. 4, but with Q_0 = 0, can characterise the pressure-dependence of the outflow facility (Fig. 7c). The reference facility predicted by the power law model is 5.3 [4.8, 5.7] nl/min/mmHg.

In order to demonstrate how this impacts estimates of facility over a large sample, we reevaluated data from 66 C57 mouse eyes described in a previous study (Sherwood et al., 2016). Fig. 7d shows a ‘Cello Plot’, statistically summarising the proportional difference between the facility estimated using linear (with Q_0 as a free parameter) and power law models. As we have shown that Q_0 = 0 and the facility varies as a function of pressure, using the linear model that does not account for these effects introduces an error in the estimation of outflow facility. The average error was 100% [88, 114 %] (mean [95% CI], indicated by the central white line and dark band respectively). The two standard deviation range covers 20–234%, meaning that for a given eye, the error introduced by incorrect use of the common linear model would result in a large but relatively unpredictable error in the estimate of facility. Although the cause of the non-linearity in the present data may be artefactual and the conditions will differ between *post mortem* and *in vivo* perfusions, some degree of nonlinearity is expected in all data as a linear relationship is a special case.

4.4 How does pressure-independent flow affect facility measurements?

Using the power law model with Q_0 as a free parameter (Eq. 4), we compared the facility between contralateral eyes, with only one eye receiving an imposed Q_0. The average fold difference between contralateral eyes was 0.98 ^{x}/1.27 (1.67), which compares well with 1.08 ^{x}/1.17 (1.57), reported in our previous study (Sherwood et al., 2016) for 10 pairs of eyes with a single cannula, following the stepping protocol used for the single cannula experiments. The two geometric standard deviation levels for the two data sets (1.67 vs 1.57) are similar, indicating that the presence of the pressure-independent flow has negligible impact on our ability to resolve facility, provided that the pressure-dependent changes in facility are accounted for, as with Eq. 4.

4.5 Towards *in vivo* measurements

For *in vivo* perfusion measurements, the episcleral vessel pressure would be non-zero, and therefore P_e would need to be measured to assess Q_0. Using the technique proposed in the present study, P could be set to P_e and Q_0 could be directly measured.

Measurement of P_e could be carried out using the method of lowering the intraocular pressure until red blood cells can be observed in Schlemm's canal (Aihara et al., 2003; Millar et al., 2011). Due to the uncertainty in measuring P_e, the acquired Q_0 measurements *in vivo* would be less accurate than in *ex vivo* measurements. Considering Eq. 1 and 2, any inaccuracy in the estimated P_e would alter the measured value of Q_0 by a factor of $C(P\text{-}P_e)$. Assuming C = 5.5 nl/min, if we could identify P_e to within ± 2 mmHg, this would correspond to an uncertainty of approximately ± 10 nl/min in the direct measurement of Q_0 (approximately a 2SD range), indicating that the approach should be robust.

For *in vivo* measurements, the >60 minutes required to measure $Q(P\rightarrow 0)$ would be significantly shortened, as at $P = P_e$, the ocular compliance would be reduced several fold compared to P = 0. Furthermore, newly available flow sensors with 150 μm inner capillaries (Sensirion SLG150) have an R_q that is sixteen-fold lower than present sensors with a 75 μm capillary. Hence, we would expect to be able to measure Q_0 within 5 minutes *in vivo*, having first determined P_e.

Limitations—A single value of pressure-independent flow was investigated, at a magnitude chosen based on various reports of mouse eyes from multiple strains and ages. However, the two standard deviation range from our data suggests that we could have measured any value of Q_0 within approximately 7 nl/min for a given eye. Further experiments requiring more animals were therefore not justified.

This study included only enucleated eyes, and thus neglects the complexity of *in vivo* AHD. We chose this approach because enucleated eyes provide a platform for validating our method to measure Q_0 that would not be possible *in vivo*. First, using enucleated eyes reduces the number of unknown parameters in Eq. 1 from three *in vivo* (C, Q_0, P_e), to *one ex vivo* (C), as we have shown that Q_0 = 0 in enucleated eyes under normal perfusion conditions. Thus, *ex vivo* measurements of C have lower uncertainty than *in vivo* measurements. Second, enucleated eyes allow us to impose a constant, known value of Q_0 and demonstrate that our method reproduces this value. *In vivo*, any potential changes in Q_{in}, Q_u or P_e, as may be caused by anaesthesia for instance, would confound any attempt at validation. Third, enucleated eyes allow tighter control of temperature and hydration, which have been shown to affect measured values of C and Q_0 (Boussommier-Calleja et al., 2015). Future studies will extend this work to *in vivo* eyes.

Conclusions

Hitherto, estimates of pressure-independent flow have been made *indirectly*, by extrapolating a (typically linear) fit to flow-pressure data. In this study, we described and tested an approach to *directly* measure pressure-independent flow in mouse eyes. Using this technique, we showed that in properly hydrated *ex vivo* mouse eyes, there is no pressure-

independent flow, in contrast to previous studies using the extrapolation approach. We then imposed a pressure-independent flow using a syringe pump and demonstrated that we could accurately measure the imposed flow rate. We further demonstrated that the presence of pressure-independent flow did not influence measurements of facility, as long as the pressure-dependence of outflow facility was considered when analysing the data. The technique validated in this study will be applicable to *in vivo* analyses, enabling the first direct pressure-independent flow measurements *in vivo*.

Supplementary Material

Refer to Web version on PubMed Central for supplementary material.

Acknowledgments

We acknowledge funding support from the BrightFocus Foundation (G2015145), National Eye Institute (EY022359) and a PhD Studentship from Fight for Sight (UK; 1385).

References

Aihara M, Lindsey JD, Weinreb RN. Aqueous humor dynamics in mice. Invest Ophthalmol Vis Sci. 2003; 44:5168–5173. [PubMed: 14638713]

Becker B, Neufeld AH. Pressure dependence of uveoscleral outflow. J Glaucoma. 2002; 11:464. [PubMed: 12362090]

Bill A, Phillips CI. Uveoscleral drainage of aqueous humour in human eyes. Exp Eye Res. 1971; 12:275–281. [PubMed: 5130270]

Boussommier-Calleja A, Bertrand J, Woodward DF, Ethier CR, Stamer WD, Overby DR. Pharmacologic manipulation of conventional outflow facility in ex vivo mouse eyes. Invest Ophthalmol Vis Sci. 2012; 53:5838–5845. [PubMed: 22807298]

Boussommier-Calleja A, Li G, Wilson A, Ziskind T, Scinteie OE, Ashpole NE, Sherwood JM, Farsiu S, Challa P, Gonzalez P, Downs JC, Ethier CR, Stamer WD, Overby DR. Physical factors affecting outflow facility measurements in mice. Invest Ophthalmol Vis Sci. 2015; 56:8331–8339. [PubMed: 26720486]

Boussommier-Calleja A, Overby DR. The influence of genetic background on conventional outflow facility in mice. Invest Ophthalmol Vis Sci. 2013; 54:8251–8258. [PubMed: 24235015]

Chandrawati R, Chang JYH, Reina-Torres E, Jumeaux C, Sherwood JM, Stamer WD, Zelikin AN, Overby DR, Stevens MM. Localized and controlled delivery of nitric oxide to the conventional outflow pathway via enzyme biocatalysis: toward therapy for glaucoma. Adv Mater. 2017; 29:1604932.

Chang JYH, Stamer WD, Bertrand J, Read AT, Marando CM, Ethier CR, Overby DR. Role of nitric oxide in murine conventional outflow physiology. Am J Physiol Cell Physiol. 2015; 309:C205–C214. [PubMed: 26040898]

Crowston JG, Aihara M, Lindsey JD, Weinreb RN. Effect of latanoprost on outflow facility in the mouse. Invest Ophthalmol Vis Sci. 2004; 45:2240–2245. [PubMed: 15223801]

Friedenwald JS. Contribution to the theory and practice of tonometry. Am J Ophthalmol. 1937; 20:985–1024.

Grant WM. Clinical measurements of aqueous outflow. AMA Arch Ophthalmol. 1951; 46:113–131. [PubMed: 14856471]

Johnson M, McLaren JW, Overby DR. Unconventional aqueous humor outflow: A review. Exp Eye Res. 2017; 158:94–111. [PubMed: 26850315]

Kaufman PL. Some thoughts on the pressure dependence of uveoscleral flow. J Glaucoma. 2003; 12:89. [PubMed: 12619645]

Kumar S, Shah S, Deutsch ER, Tang HM, Danias J. Triamcinolone acetonide decreases outflow facility in C57BL/6 mouse eyes. Invest Ophthalmol Vis Sci. 2013; 54:1280–1287. [PubMed: 23322580]

Lei Y, Overby DR, Boussommier-Calleja A, Stamer WD, Ethier CR. Outflow physiology of the mouse eye: pressure dependence and washout. Invest Ophthalmol Vis Sci. 2011; 52:1865–1871. [PubMed: 21169533]

Li G, Farsiu S, Chiu SJ, Gonzalez P, Lütjen-Drecoll E, Overby DR, Stamer WD. Pilocarpine-induced dilation of Schlemm's canal and prevention of lumen collapse at elevated intraocular pressures in living mice visualized by OCT. Invest Ophthalmol Vis Sci. 2014; 55:3737–3746. [PubMed: 24595384]

Li G, Mukherjee D, Navarro I, Ashpole NE, Sherwood JM, Chang J, Overby DR, Yuan F, Gonzalez P, Kopczynski CC, Farsiu S, Stamer WD. Visualization of conventional outflow tissue responses to netarsudil in living mouse eyes. Eur J Pharmacol. 2016; 787:20–31. [PubMed: 27085895]

Millar JC, Clark AF, Pang IH. Assessment of aqueous humor dynamics in the mouse by a novel method of constant-flow infusion. Invest Ophthalmol Vis Sci. 2011; 52:685–694. [PubMed: 20861483]

Millar JC, Phan TN, Pang IH, Clark AF. Strain and age effects on aqueous humor dynamics in the mouse. Invest Ophthalmol Vis Sci. 2015; 56:5764–5776. [PubMed: 26325415]

Overby DR, Bertrand J, Schicht M, Paulsen F, Stamer WD, Lütjen-Drecoll E. The structure of the trabecular meshwork, its connections to the ciliary muscle, and the effect of pilocarpine on outflow facility in mice. Invest Ophthalmol Vis Sci. 2014a; 55:3727–3736. [PubMed: 24833737]

Overby DR, Bertrand J, Boussommier-Calleja A, Tektas OY, Schicht M, Ethier CR, Stamer WD, Woodward DF, Lütjen-Drecoll E. Ultrastructural changes associated with dexamethasone-induced ocular hypertension in mice. Invest Ophthalmol Vis Sci. 2014b; 55:4922–4933. [PubMed: 25028360]

O'Callaghan J, Crosbie DE, Cassidy PS, Sherwood JM, Flügel-Koch C, Lütjen-Drecoll E, Humphries MM, Reina-Torres E, Wallace D, Kiang AS, Campbell M, Stamer WD, Overby DR, O'Brien C, Tam LCS, Humphries P. Therapeutic potential of AAV-mediated MMP-3 secretion from corneal endothelium in treating glaucoma. Hum Mol Genet. 2017; 26:1230–1246. [PubMed: 28158775]

Reina-Torres E, Wen JC, Liu KC, Li G, Sherwood JM, Chang JYH, Challa P, Flügel-Koch CM, Stamer WD, Allingham RR, Overby DR. VEGF as a paracrine regulator of conventional outflow facility. Invest Ophthalmol Vis Sci. 2017; 58:1899–1908. [PubMed: 28358962]

Resnikoff S, Pascolini D, Etyaale D, Kocur I, Pararajasegaram R, Pokharel GP, Mariotti SP. Global data on visual impairment in the year 2002. Bull World Health Organ. 2004; 82:844–851. [PubMed: 15640920]

Rogers ME, Navarro ID, Perkumas KM, Niere SM, Allingham RR, Crosson CE, Stamer WD. Pigment epithelium-derived factor decreases outflow facility. Invest Ophthalmol Vis Sci. 2013; 54:6655–6661. [PubMed: 24030458]

Sherwood JM, Reina-Torres E, Bertrand JA, Rowe B, Overby DR. Measurement of outflow facility using iPerfusion. PLoS One. 2016; 11:e0150694. [PubMed: 26949939]

Stamer WD, Acott TS. Current understanding of conventional outflow dysfunction in glaucoma. Curr Opin Ophthalmol. 2012; 23:135–143. [PubMed: 22262082]

Tam LCS, Reina-Torres E, Sherwood JM, Cassidy PS, Crosbie DE, Lütjen-Drecoll E, Flügel-Koch C, Perkumas K, Humphries MM, Kiang AS, O'Callaghan J, Callanan JJ, Read AT, Ethier CR, O'Brien C, Lawrence M, Campbell M, Stamer WD, Overby DR, Humphries P. Enhancement of outflow facility in the murine eye by targeting selected tight-junctions of Schlemm's canal endothelia. Sci Rep. 2017; 7:40717. [PubMed: 28091584]

Toris CB, Fan S, Johnson TV, Camras LJ, Hays CL, Liu H, Ishimoto BM. Aqueous flow measured by fluorophotometry in the mouse. Invest Ophthalmol Vis Sci. 2016; 57:3844–3852. [PubMed: 27447085]

Toris CB, Gleason ML, Camras CB, Yablonski ME. Effects of brimonidine on aqueous humor dynamics in human eyes. Arch Ophthalmol. 1995; 113:1514–1517. [PubMed: 7487618]

Townsend DJ, Brubaker RF. Immediate effect of epinephrine on aqueous formation in the normal human eye as measured by fluorophotometry. Invest Ophthalmol Vis Sci. 1980; 19:256–266. [PubMed: 7358476]

Van Veldhuisen PC, Ederer F, Gaasterland DE, Sullivan EK, Beck AD, Prum BE Jr, Cyrlin MN, Weiss H. The advanced glaucoma intervention study (AGIS): 7. The relationship between control of intraocular pressure and visual field deterioration. Am J Ophthalmol. 130:429–440.

Wang K, Read AT, Sulchek T, Ethier CR. Trabecular meshwork stiffness in glaucoma. Exp Eye Res. 2017; 158:3–12. [PubMed: 27448987]

Zhang D, Vetrivel L, Verkman AS. Aquaporin deletion in mice reduces intraocular pressure and aqueous fluid production. J Gen Physiol. 2002; 119:561–569. [PubMed: 12034763]

Zhang Y, Davidson BR, Stamer WD, Barton JK, Marmorstein LY, Marmorstein AD. Enhanced inflow and outflow rates despite lower IOP in bestrophin-2-deficient mice. Invest Ophthalmol Vis Sci. 2009; 50:765–770. [PubMed: 18936135]

Highlights

- We report the first *direct* measurement of net pressure-independent AH flow (Q_0).
- Q_0 is the difference between aqueous humour inflow and pressure-independent outflow.
- In enucleated mouse eyes, $Q_0 = 0$, in contrast with previous estimates.
- When a known Q_0 is imposed, we can measure it accurately (within 10 nl/min).
- Inaccurate assessment of Q_0 leads to significant errors when measuring facility.

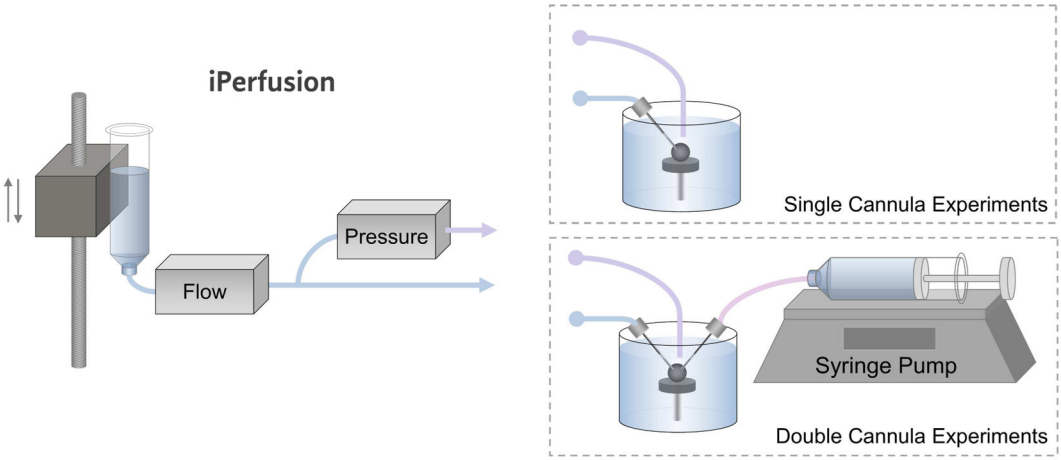

Fig. 1.

Schematic of the experimental setup. The *iPerfusion* system comprises an actuated reservoir to control the applied pressure, a thermal flow sensor to measure the flow rate from the reservoir, and a differential pressure sensor to measure the pressure in the eye with respect to the bath. For the single cannula experiments, the eye was cannulated with one glass needle connected to *iPerfusion*. For the double cannula experiments, the eye was cannulated with two glass needles, connecting it to both the *iPerfusion* system and a syringe pump, used to impose a known pressure-independent flow.

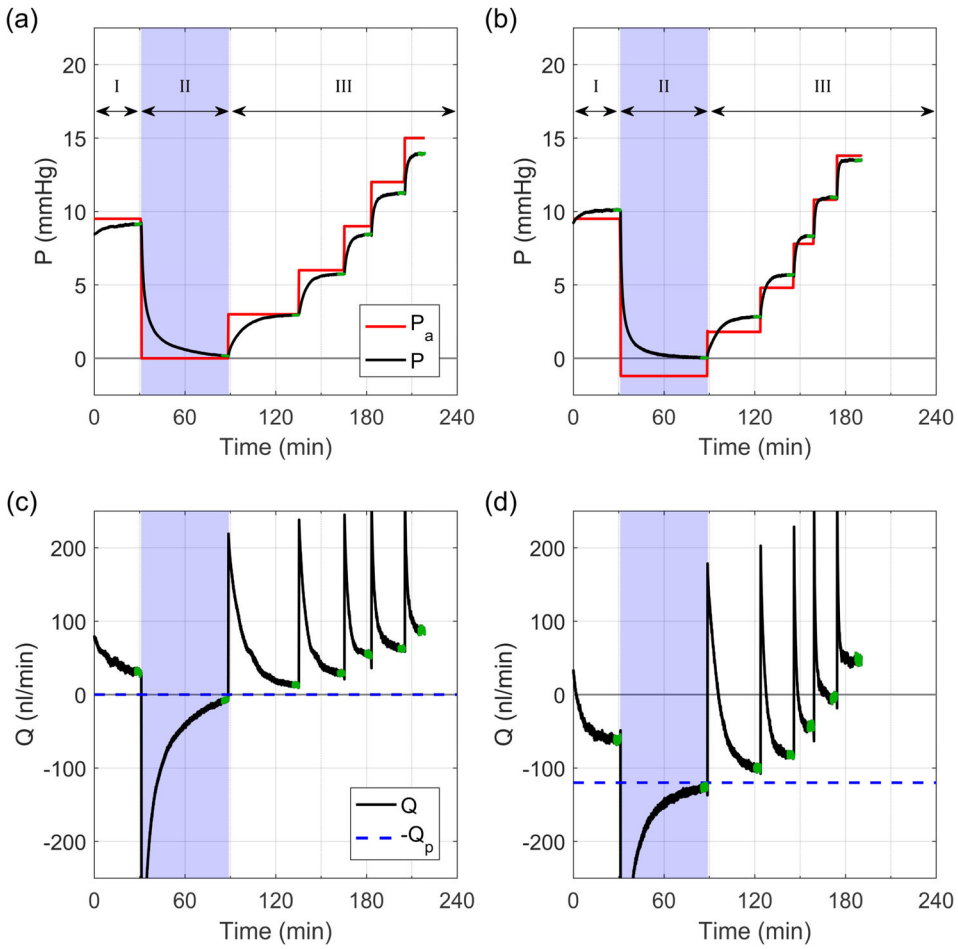

Fig. 2.

Flow (*Q*) and pressure (*P*) traces from a typical perfusion from the double cannula experiments. Traces (a) and (c) correspond to recordings from a control eye with Q_p = 0 nl/min, while (b) and (d) correspond to recordings from the contralateral experimental eye with Q_p = 120 nl/min. Green regions indicate steady state. Note that the difference between P_a and *P* arises from the resistance of the flow sensor, R_q, and the compliance of the eye.

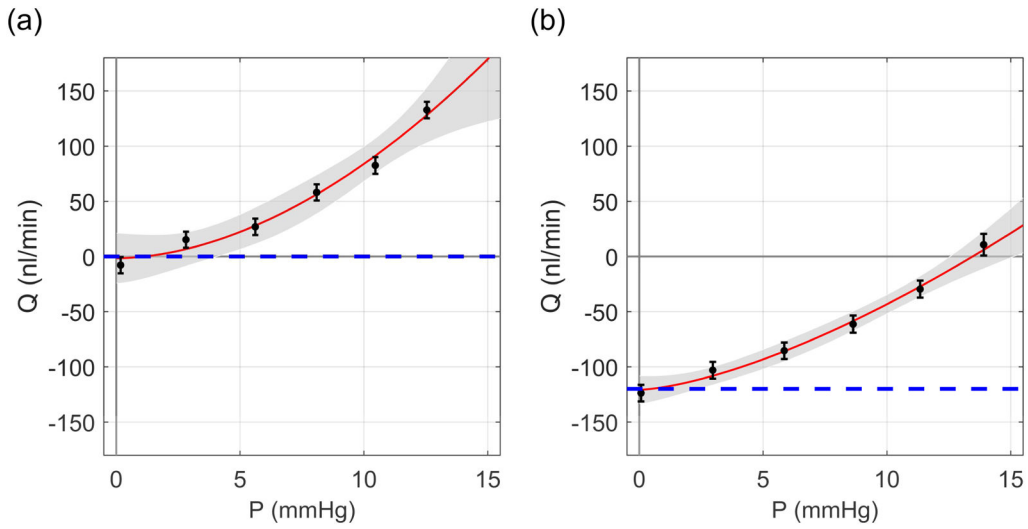

Fig. 3.

Sample flow-pressure plots. (a) Control eye with Q_p = 0 nl/min and (b) the contralateral experimental eye with Q_p = 120 nl/min. Dashed lines illustrate $-Q_p$. Red curves represent the best fit of Eq. 4 to the flow-pressure data, with the 95% confidence intervals shown in grey. Error bars represent two standard deviations.

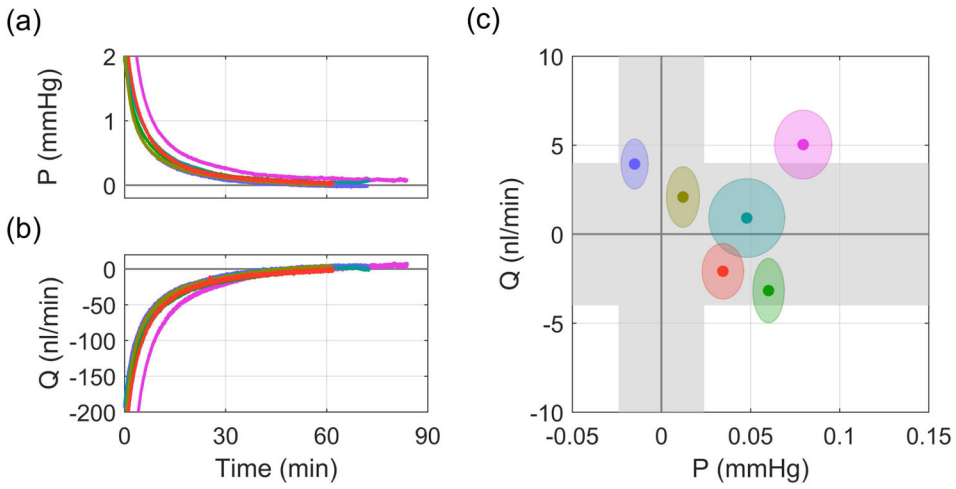

Fig. 4.

Direct measurement of $Q(P \rightarrow 0)$ in the single cannula experiments. (a) Pressure and (b) flow traces after P_a was set to 0 mmHg. (c) Steady state values of pressure and flow. Grey regions indicate sensor uncertainty and ellipses show two standard deviations on the recorded flow and pressure signals.

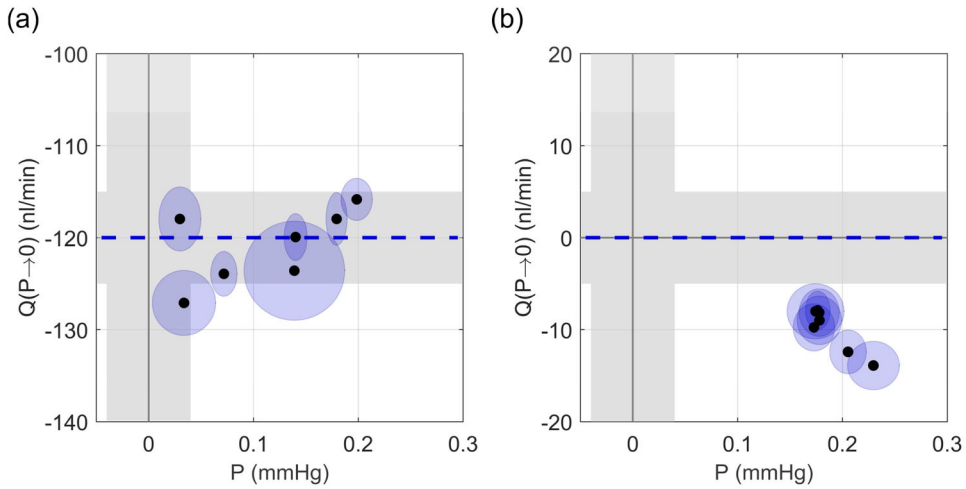

Fig. 5.

Direct measurement of $Q(P \rightarrow 0)$ from Phase II of the double cannula experiments. (a) Experimental eyes with Q_p = 120 nl/min, (b) control eyes with Q_p = 0 nl/min. Grey regions indicate sensor uncertainty and ellipses show two standard deviations. Dashed blue line indicates $-Q_p$.

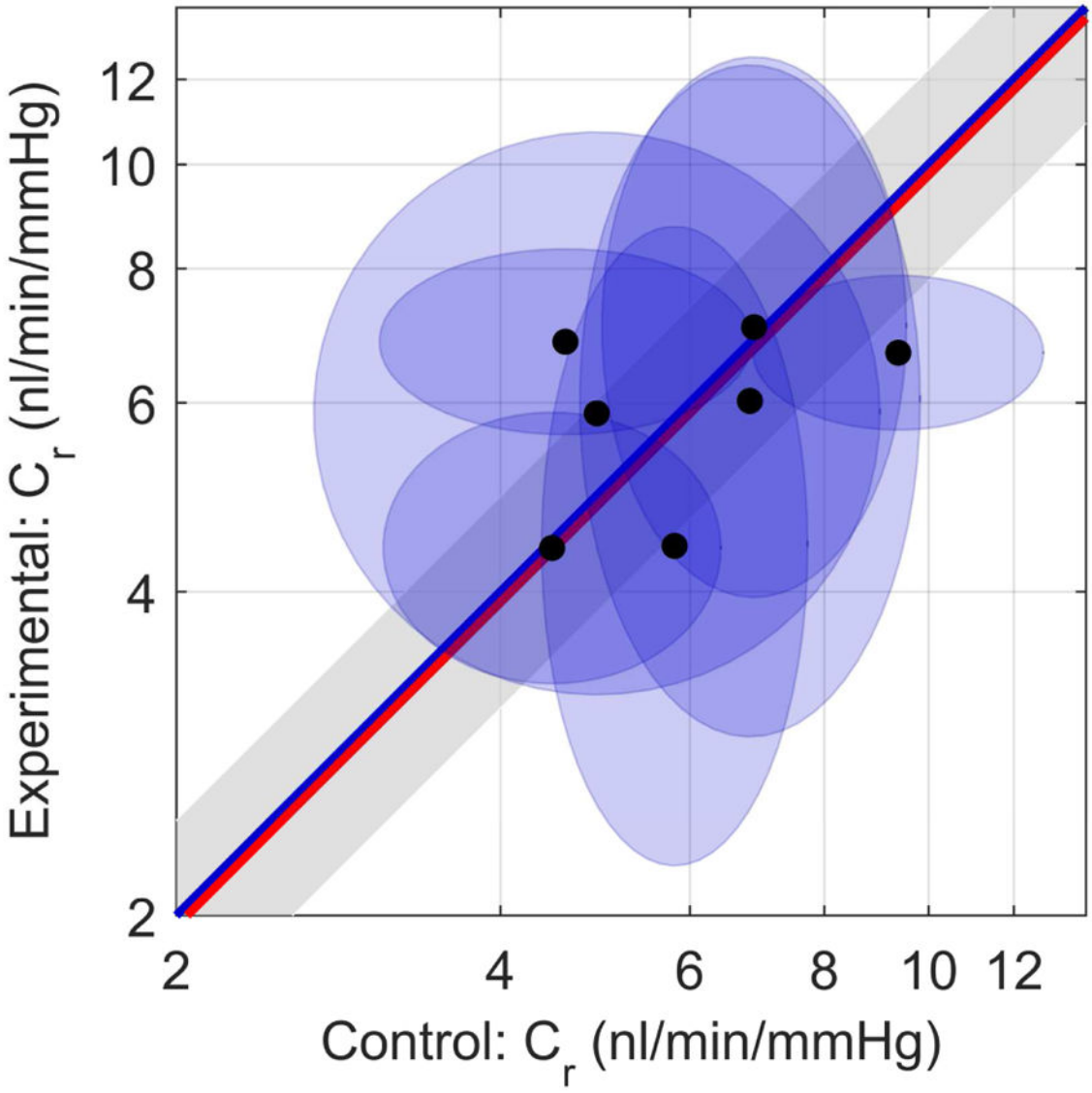

Fig. 6.

Paired plot of reference facility C_r. Control eyes (Q_p = 0 nl/min along x-axis), Experimental eyes (Q_p = 120 nl/min along y-axis). Each data point represents one mouse, and ellipses indicate 95% confidence intervals on C_r. The blue unity line represents the ideal case of perfect agreement in C_r between contralateral eyes, while the red line indicates the mean difference in measured facility between paired eyes. The grey shaded region indicates the confidence interval on the mean difference.

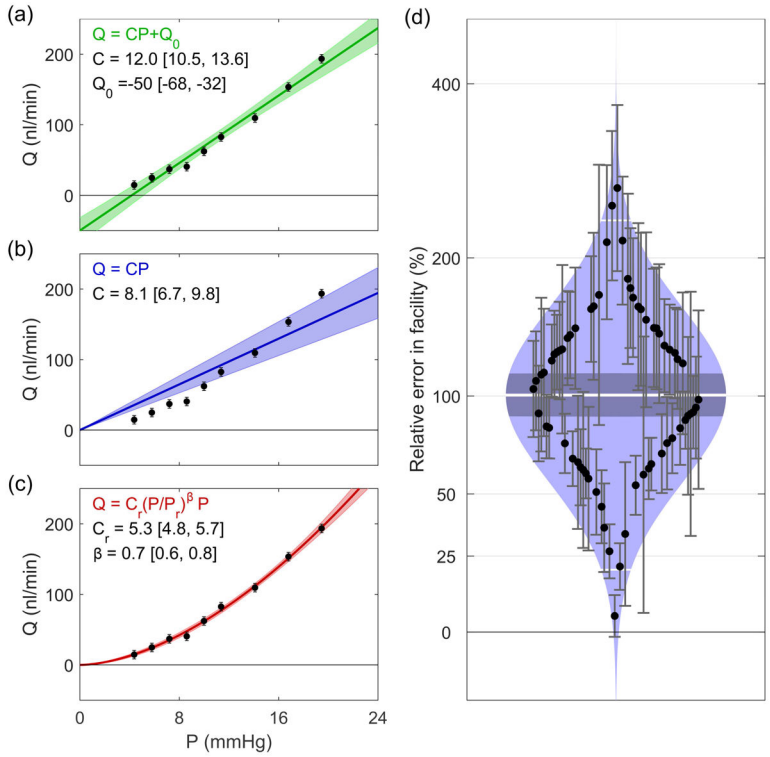

Fig. 7.

Comparison of models for fitting flow-pressure data. (a) Common linear model, (b) linear model with zero intercept, (c) power law model. Shaded regions indicate the 95% confidence intervals of the fits. (d) Cello plot showing relative error in estimates of facility when using the common linear model. Shaded regions indicate predicted lognormal distribution, with the mean (central white line), confidence interval on the mean (central dark band), and ± two standard deviations around the mean (outer white lines). Each data point shows an individual eye and error bars indicate the 95% confidence interval on the relative error. Data reprocessed from (Sherwood et al., 2016).